

Inhibition of Non-Essential Bacterial Targets: Discovery of a Novel Serine *O*-acetyltransferase Inhibitor

Joana Magalhães,^a Nina Franko,^b Samanta Raboni,^{b,f} Giannamaria Annunziato,^a Päivi Tammela,^c
Agostino Bruno,^{a,†} Stefano Bettati,^{d,e,f} Andrea Mozzarelli,^{b,e,f} Marco Pieroni,^{a,g,*} Barbara
Campanini,^b Gabriele Costantino^{a,g,h}

^a*P4T group, and* ^b*Laboratory of Biochemistry and Molecular Biology Department of Food and Drug, University of Parma, 43124 Parma, Italy;* ^c*Drug Research Program, Division of Pharmaceutical Biosciences, Faculty of Pharmacy, University of Helsinki, P.O. Box 56 (Viikinkaari 5 E), Helsinki, FI-00014, Finland;* ^d*Department of Medicine and Surgery, University of Parma, 43125 Parma, Italy;* ^e*National Institute of Biostructures and Biosystems, Rome, Italy;* ^f*Institute of Biophysics, CNR, Pisa, Italy;* ^g*Centro Interdipartimentale “Biopharmanet-tec”, Università degli Studi di Parma, Parma, Italy;* ^h*Centro Interdipartimentale Misure (CIM) ‘G. Casnati’, University of Parma, Parma, Italy.*
[†]*Present address: Experimental Therapeutics Program, IFOM – The FIRC Institute for Molecular Oncology Foundation, Via Adamello 16-20139, Milano, Italy.*

Supporting information

<i>Virtual screening</i>	Pag 2
<i>Protein expression and purification</i>	Pag 4
<i>Determination of StSAT inhibition</i>	Pag 5
<i>Evaluation of MIC</i>	Pag 6
<i>Chemistry and synthesis of compound 3</i>	Pag 7
<i>Structures of compounds from VS and % Inhibition</i>	Pag 8

Experimental procedures

Virtual screening

X-ray structure selection and preparation

For this study, we decided to use the X-ray crystal structures of the WT *EcSAT* in complex with cysteine (1T3D) and the structure of WT *HiSAT* in complex with CoA (1SSM). This decision was dictated by two relevant aspects: (i) *EcSAT* and *HiSAT* share with *StSAT* a sequence identity of the 100% at the active site level; (ii) *EcSAT* and *HiSAT* being bound to cysteine and CoA show subtle conformational differences at the active site level. Both X-ray crystal structure were prepared using the protein preparation wizard available in Maestro, which assigns bond orders, adds hydrogen atoms, deletes water molecules, and generates appropriate protonation states (<https://www.schrodinger.com>). The docking grid boxes for both 1T3D and 1SSM were centred in such a way to include all the residues into a 4-Å shell around the substrate cysteine bound in the 1T3D X-ray, with a box size of 26 x 26 x 26 Å³.

Libraries preparation

The sd file of 2-D structures of the compounds were retrieved from the ChemDiv Anti-infective (8523), anti-bacterial (5460), and antiviral (77260) focused library collections, for a total of 91243 compounds. Libraries were merged using Canvas (<https://www.schrodinger.com>) and duplicates were removed. Hydrogen atoms, protonation states at pH 7.4, 3-D conversion of the structures and conformational search were performed at the initial stages of the Virtual Screening Workflow (vsw) available in Maestro by using LigPrep (<https://www.schrodinger.com>). PhysChem properties and related filters such as Lipinski's Rule, reactive functional groups were evaluated by using QuickProp (<https://www.schrodinger.com>).

Virtual Screening Workflow

Virtual screening was performed by using the multigrid option of the vsw panel available in Maestro. Vsw allowed us to carry out a 3 steps virtual screening. In the first step the HTSV option was used in order to generate as much as possible binding poses for each ligand and the 75% of the best scoring compounds was retained. During the second step, the generated binding poses were refined by using the SP method available in Glide (<https://www.schrodinger.com>) and three binding modes per ligand were generated. In this case, only the 75% of the best scoring compounds was retained. Finally, for each compound a MM-GBSA rescoring protocol was performed, considering for each compound the three binding modes previously generated. In

such a way, we were able to identify the most energetically favorable binding mode for each ligand, and only the top 2.75% of the best scoring compounds was retained, leading to the selection of the final 1.409 virtual hits to be further evaluated by visual inspection.

Protein expression and purification

The *StSAT* expression vector was generated by insertion of the synthetic gene (GeneArt, ThermoFisher, Waltham, MA USA 02451) into the pSH21p-His6-trxA plasmid (a kind gift from Professor Christopher S. Hayes, MCDB, University of California, Santa Barbara), replacing the insert for *E. coli* SAT. Nucleotide sequence of SAT from *S. Typhimurium*, obtained from Uniprot (entry A0A0U1JK50), was optimized for expression in *E. coli*. The sequence of the new construct was confirmed by sequencing reaction. The expression vector was transformed into competent *E. coli* Tuner™ BL21(DE3) cells (Novagen, Merck Biosciences, Billerica, MA, USA) by electroporation. *StSAT* was expressed and purified as previously described for *EcSAT*¹ with few changes. Briefly, *E. coli* Tuner™ cells transformed with the expression vector were grown overnight and diluted 1:100 in LB added of 150 µg/mL ampicillin and 1 % glucose. Cells were grown at 37 °C and 250 RPM until the midlog phase and induced with 1 mM IPTG for 4 hours. Cells were pelleted and stored at -80 °C. The cell pellet was resuspended in lysis buffer (100 mM Tris, 500 mM NaCl, 50 mM imidazole, 50 µM L-cysteine, 1 mM TCEP, pH = 7.5) in presence of 1 mg/mL lysozyme, 0.2 mM PMSF, 0.2 mM benzamidine and 1.5 µM pepstatin A. Cells were then lysed by pulsed sonication and the protein purified by affinity chromatography on Talon™ resin (Clontech Laboratories, Inc., Mountain View, CA, USA). Endogenous *O*-acetylserine sulfhydrylase bound to SAT was eluted with 10 mM OAS. *StSAT* was eluted with imidazole and the His₆-trxA tag was cleaved by *in house* produced TEV protease. TEV protease, the cleaved tag and high molecular weight aggregates were removed by size exclusion chromatography using HiLoad 16/600 Superdex 75 prep grade column. The final enzyme preparation was more than 95 % pure based on the SDS-PAGE analysis. *StSAT* concentration was calculated by using an extinction coefficient $\epsilon_{280}=26930 \text{ M}^{-1} \text{ cm}^{-1}$.

Determination of *Sr*SAT inhibition

*Sr*SAT inhibitory activity of the 73 commercial compounds acquired was evaluated using an indirect continuous assay (Scheme 1). The assay was previously optimized at 20 °C in a cuvette-format using a Cary 4000 UV-Vis spectrophotometer (Agilent, Santa Clara, CA, USA) equipped with a cuvette holder thermostated through a circulating water bath. The K_m and k_{cat} for both substrates and the IC_{50} for the inhibitor glycine were calculated and compared with data obtained using the direct continuous assay. The assay buffer was 20 mM sodium phosphate, 85 mM NaCl, 1 mM EDTA, pH 7. The enzyme concentration was 7 nM and the concentration of DTNB was 1 mM. The concentration of acetyl-CoA for the determination of the catalytic parameters for L-Ser was 0.25 mM, the concentration of L-Ser was 1 mM. For the determination of the IC_{50} for glycine, the concentration of the substrates was 0.25 mM and 1 mM for acetyl-CoA and L-Ser, respectively. In all cases, the reaction was initiated by addition of acetyl-CoA to the reaction mixture. The optimized assay was transferred into a 96-well plate format. The only difference with respect to the assay carried out in cuvettes was the addition to the enzyme dilution of 100 µg/mL bovine serum albumin (BSA) and 15% glycerol. The total volume in each well was 200 µL. The absorbance was read at 412 nm using a Multiskan Go plate reader (Thermo Fisher Scientific, Finland). The plates were measured 12 times: first one background determination and then every 27s during about 5 min. The reaction was started with the addition of the substrate acetyl-CoA and % of inhibition for each compound was calculated at time-point 180s, which was selected as the endpoint based on assay quality parameters S/B, SW and Z'. First, the inhibitory potency against *Sr*SAT was tested at 100 µM, then compounds with a percentage of inhibition equal or higher than 40% were re-tested at the same concentration. Finally, dose-response curves were performed to determine IC_{50} for all the compounds that showed a percentage of inhibition higher than 50% in the two screenings at 100 µM.

Evaluation of MIC

Minimal inhibitory concentration (MIC) was determined by the broth microdilution assay according to CLSI guidelines.² Briefly, *E. coli* ATCC25922 (obtained from Microbiologics Inc., USA) was grown at 37°C on MHB agar plates for 16-24h. A loopful of bacteria was transferred into 5 mL saline and the turbidity of the suspension was measured with a densitometer, and suspension with 1×10^6 colony-forming units (CFU)/mL was prepared into assay media. Compounds were dissolved in DMSO and 2-fold dilution series (10 concentrations) starting from 128 µg/mL were prepared. Ciprofloxacin was used as standard antibiotic and each plate contained growth control wells and sterility check wells. The plates were incubated at 37°C for 16h-24h and MIC was defined as the lowest concentration at which the bacterial growth was inhibited by >90%.

References

- (1) Benoni, R.; Bei, O. D.; Paredi, G.; Hayes, C. S.; Franko, N.; Mozzarelli, A.; Bettati, S.; Campanini, B. Modulation of Escherichia Coli Serine Acetyltransferase Catalytic Activity in the Cysteine Synthase Complex. *FEBS Lett.* 2017, 591 (9), 1212–1224. <https://doi.org/10.1002/1873-3468.12630>.
- (2) CLSI, *Methods for Dilution Antimicrobial Susceptibility Tests for Bacteria That Grow Aerobically*, Approved Standard—Ninth Edition, CLSI document - (accessed Dec 14, 2019).

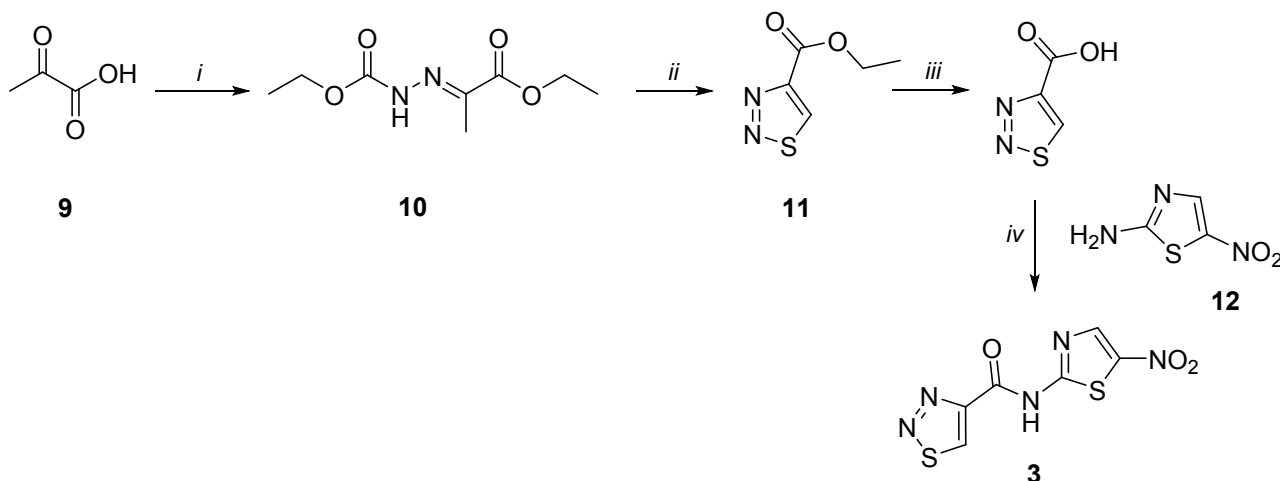
Chemistry and synthesis of compound 3

Chemistry

Compound **3** was resynthesized in order to confirm the previously obtained results with the commercial sample (Scheme 2). Briefly, 1,2,3-thiadiazole-4-carboxylic acid was synthesized as previously reported starting from pyruvic acid that gives hydrazone **10** upon treatment with SOCl_2 and ethyl hydrazinecarboxylate in ethanol.³ Ethyl 2-(1-ethoxy-1-oxopropan-2-ylidene)hydrazinecarboxylate is then reacted with SOCl_2 to give ethyl 1,2,3-thiadiazole-4-carboxylate **11** in good yield, that is hydrolyzed to the corresponding acid. Acid **11** is activated with 1,1'-Carbonyldiimidazole (CDI) for 1h and then 4-nitrothiazol-2-amine was added to the reaction mixture to give compound **3** in good yields. HRMS (ESI) calculated for $\text{C}_6\text{H}_3\text{N}_5\text{O}_3\text{S}_2$ $[\text{M} + \text{H}]^+$ 257,9677, found 257.9589

Compounds **3-8** were tested as 95–100% purity samples (by HPLC/MS). HPLC/MS experiments were performed with HPLC: Agilent 1100 series, equipped with a Waters Symmetry C18, 3.5 μm , 4.6 mm x 75 mm column and MS: Applied Biosystem/MDS SCIEX, with API 150EX ion source. HRMS experiments were performed with LTQ ORBITRAP XL THERMO.

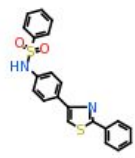
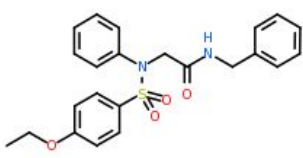

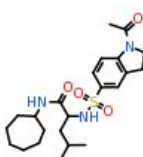
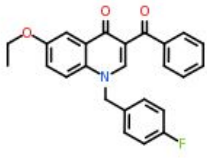
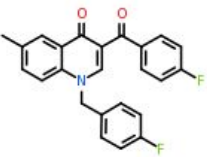
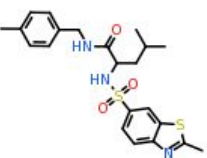
Scheme 2^a Synthesis of compound 3

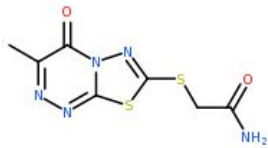
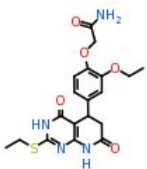
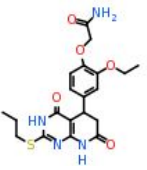
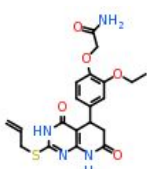
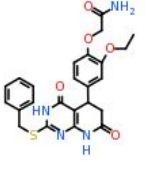
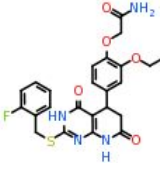
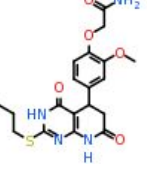
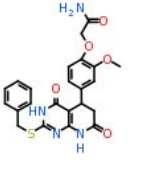




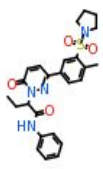
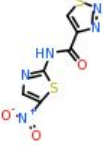
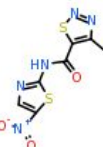
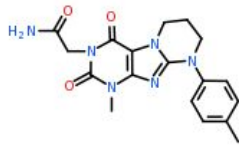
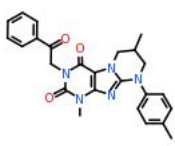
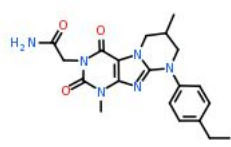
^aReagents and conditions: *i*) EtOH, SOCl_2 , ethyl hydrazinecarboxylate, 61%; *ii*) DCM, SOCl_2 ; 39%; *iii*) NaOH 2N, MeOH; 38%; *iv*) CDI, DMF, 4-nitrothiazol-2-amine, 15%.

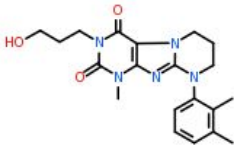
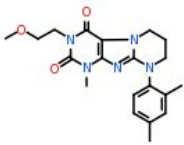
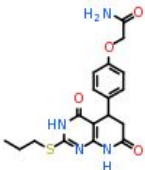
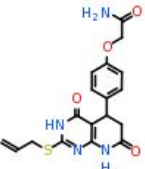
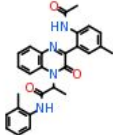
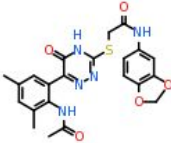
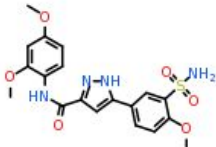
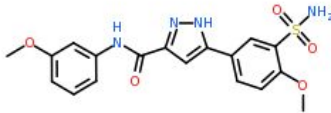
(3) Hurd, C. D.; Mori, R. I. On Acylhydrazones and 1,2,3-Thiadiazoles. *J. Am. Chem. Soc.* **1955**, 77 (20), 5359–5364. <https://doi.org/10.1021/ja01625a047>.

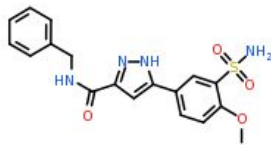

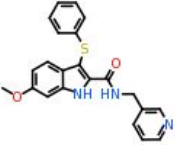
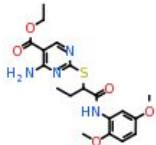
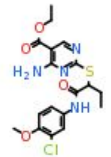
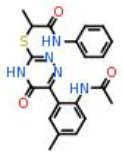
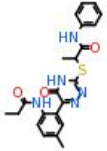
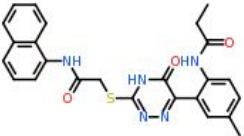
Structures of compounds from VS

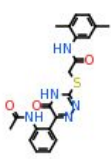
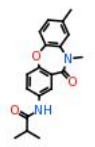
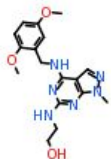
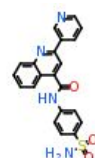
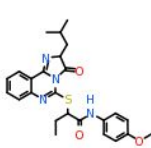
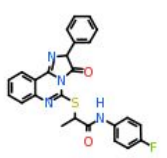
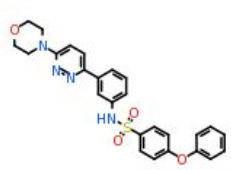
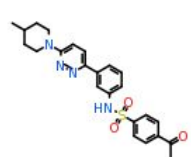
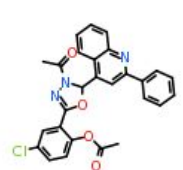
Compound ID	Molecular formula	Structure	% inhibition @ 100 μ M
3382-1221	C ₂₁ H ₁₆ N ₂ O ₂ S ₂		22,20082018
4577-0157	C ₂₃ H ₂₄ N ₂ O ₄ S		60,09071704
4577-2315	C ₂₂ H ₂₂ N ₂ O ₃ S		29,94904934
C450-0514	C ₂₃ H ₃₅ N ₃ O ₄ S		39,18230396
C567-0505	C ₂₅ H ₂₀ FNO ₃		21,17559339
C567-0562	C ₂₄ H ₁₇ F ₂ NO ₂		45,30881074
C583-0084	C ₂₂ H ₂₇ N ₃ O ₃ S ₂		19,51451887

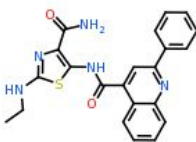
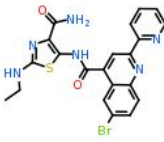
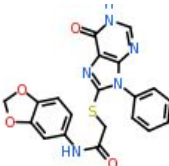
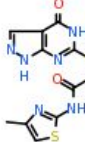
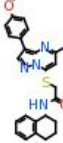
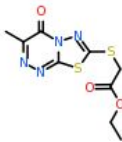
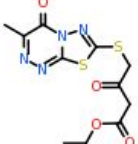
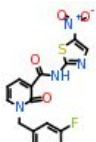
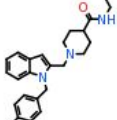
D035-0097	C7H7N5O2S2		15,90965577
D271-0196	C19H22N4O5S		-6,84105878
D271-0197	C20H24N4O5S		16,5154716
D271-0198	C20H22N4O5S		-13,78774699
D271-0201	C24H24N4O5S		47,25984839
D271-0206	C24H23FN4O5S		39,66695663
D271-0344	C19H22N4O5S		11,28785054
D271-0348	C23H22N4O5S		42,10886044

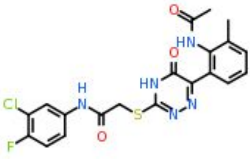
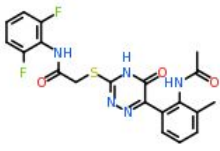
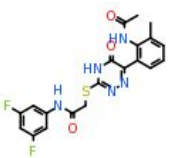
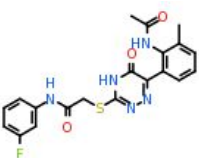
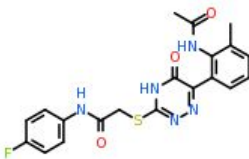
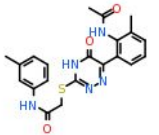

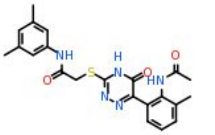
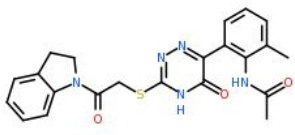
D271-0352	C23H21FN4O5S		53,14195767
D271-0353	C23H21FN4O5S		20,59773829
D315-1293	C25H28N4O4S		27,32074065
D319-0482	C6H3N5O3S2		86,19998813
D319-0733	C7H5N5O3S2		84,67935518
D389-0064	C18H20N6O3		-21,70918896
D389-0402	C25H25N5O3		14,0952776
D389-0566	C20H24N6O3		-16,05890894

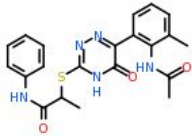
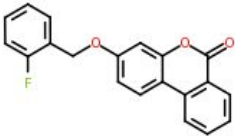
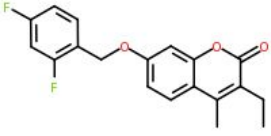
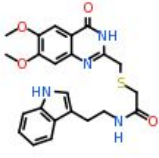

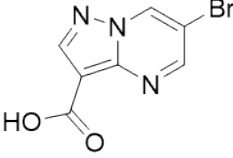
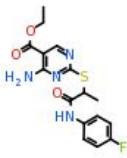
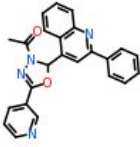
D389-1113	C ₂₀ H ₂₅ N ₅ O ₃		-25,24372537
D389-1155	C ₂₀ H ₂₅ N ₅ O ₃		-11,64488695
D392-0248	C ₁₈ H ₂₀ N ₄ O ₄ S		35,99668119
D392-0319	C ₁₈ H ₁₈ N ₄ O ₄ S		66,23107239
D395-0021	C ₂₇ H ₂₆ N ₄ O ₃		8,276291226
D509-0021	C ₂₂ H ₂₁ N ₅ O ₅ S		-8,433934868
D511-0020	C ₁₉ H ₂₀ N ₄ O ₆ S		51,23003526
D511-0060	C ₁₈ H ₁₈ N ₄ O ₅ S		77,50674134

D511-0063	C ₁₈ H ₁₈ N ₄ O ₄ S		72,28790707
D715-1491	C ₂₁ H ₁₉ NO ₇		22,67164489
E018-1781	C ₂₂ H ₁₉ N ₃ O ₂ S		-18,16635553
E726-0325	C ₁₉ H ₂₄ N ₄ O ₅ S		-3,356150176
E726-0340	C ₁₈ H ₂₁ ClN ₄ O ₄ S		12,80647169
F151-0066	C ₂₁ H ₂₁ N ₅ O ₃ S		-8,442231902
F151-0171	C ₂₂ H ₂₃ N ₅ O ₃ S		20,6388716
F151-0200	C ₂₅ H ₂₃ N ₅ O ₃ S		48,35926156

F151-0341	C21H21N5O3S		-43,01597179
F731-0396	C19H20N2O3		-7,104125953
G414-1520	C17H22N6O3		-38,38870386
G547-0536	C21H16N4O3S		-8,904241557
G568-0166	C25H28N4O3S		24,14191737
G568-0266	C25H19FN4O2S		32,41033828
G620-0245	C26H24N4O4S		24,8355399
G620-0334	C24H26N4O3S		27,14761498
G642-7235	C27H20ClN3O4		8,161074564

G748-0005	C22H19N5O2S		-5,254465883
G748-0011	C21H17BrN6O2S		-22,84825631
G754-0211	C20H15N5O4S		38,05840742
G786-1280	C11H10N6O2S2		-1,505601277
G788-0625	C26H26N4O2S		21,53257549
G856-3815	C9H10N4O3S2		-19,73245988
G856-3819	C11H12N4O4S2		-6,872918444
G857-0596	C16H11FN4O4S		-6,085711926
G907-1063	C25H31N3O		14,49175635

J041-0001	C20H17ClFN5O3S		8,612479701
J041-0002	C20H17F2N5O3S		1,654234676
J041-0004	C20H17F2N5O3S		-2,760727753
J041-0011	C20H18FN5O3S		-6,764229998
J041-0012	C20H18FN5O3S		-22,25844623
J041-0024	C21H21N5O3S		-2,238643773
J041-0026	C21H21N5O3S		-18,8920283
J041-0040	C22H23N5O3S		3,112849864
J041-0057	C22H21N5O3S		27,79830472

J041-0062	C ₂₁ H ₂₁ N ₅ O ₃ S		-9,237122365
Y040-1915	C ₂₀ H ₁₃ FO ₃		21,83341786
Y040-2426	C ₁₉ H ₁₆ F ₂ O ₃		11,444372
Y041-3100	C ₂₃ H ₂₄ N ₄ O ₄ S		36,28921249
Z601-7550	C ₁₇ H ₁₇ N ₃ O ₂		5,812746021
D717-0037	C ₇ H ₄ BrN ₃ O ₂		-15,59805839
E726-0389	C ₁₆ H ₁₇ FN ₄ O ₃ S		-7,324494675
G642-7324	C ₂₄ H ₁₈ N ₄ O ₂		-40,70854162